NAVAL POSTGRADUATE SCHOOL
Monterey, California

Approved for public release: distribution unlimited

NAVAL POSTGRADUATE SCHOOL
Monterey, California 93943

Rear Admiral R. C. Austin   D. A. Schrady
Superintendent   Provost

    This report was prepared by:

REPORT DOCUMENTATION PAGE

1 REPORT SECURITY CLASSIFICATION UNCLASSIFIED	1b RESTRICTIVE MARKINGS none
2a SECURITY CLASSIFICATION AUTHORITY	3 DISTRIBUTION/AVAILABILITY OF REPORT Approved for public release; distribution unlimited.
2b DECLASSIFICATION/DOWNGRADING SCHEDULE	

4 PERFORMING ORGANIZATION REPORT NUMBER(S) Naval Postgraduate School NPS 62-87-014	5 MONITORING ORGANIZATION REPORT NUMBER(S)

6a NAME OF PERFORMING ORGANIZATION Naval Postgraduate School	6b OFFICE SYMBOL (If applicable) Code 62	7a NAME OF MONITORING ORGANIZATION

6c ADDRESS (City, State, and ZIP Code) Monterey, California 93943-5000	7b. ADDRESS (City, State, and ZIP Code)

8a NAME OF FUNDING/SPONSORING ORGANIZATION Joint Director of Laboratories	8b OFFICE SYMBOL (If applicable)	9 PROCUREMENT INSTRUMENT IDENTIFICATION NUMBER N6600187WR00250

8c ADDRESS (City, State, and ZIP Code) JSC, Code 421 San Diego, CA 92152-5000	10 SOURCE OF FUNDING NUMBERS			
	PROGRAM ELEMENT NO 35108K	PROJECT NO RDDA	TASK NO.	WORK UNIT ACCESSION NO

11 TITLE (Include Security Classification)

Characteristic Trajectories of Generalized Lanchester Equations

12 PERSONAL AUTHOR(S)
John M. Wozencraft and Paul H. Moose

13a TYPE OF REPORT Technical	13b TIME COVERED FROM _____ TO _____	14 DATE OF REPORT (Year, Month, Day)	15 PAGE COUNT

16 SUPPLEMENTARY NOTATION

COSATI CODES			18 SUBJECT TERMS (Continue on reverse if necessary and identify by block number)
FIELD	GROUP	SUB-GROUP	Combat dynamics - non-linear, systems, heterogeneous force compositions, Mixed Attrition Lanchester with Resupply

19 ABSTRACT (Continue on reverse if necessary and identify by block number)

Generalized Lanchester-type differential equations are used to model attrition processes. This system of non-linear equations has multiple equilibrium solutions, which can be determined by a numerical technique called the Continuation Method when the problem's dimensionality is moderate.

System dynamics are investigated and shown to depend critically on a domain of attraction defined by a tube which connects the non-negative equilibrium points and contains the dominant eigenvector at those points. Principles are presented and illustrated for mapping NM-dimensional systems into equivalent two-dimensional systems. This capability is especially important when aggregating subsystems in multi-level systems modeling. It is shown that the two-dimensional Lanchester systems have only four distinct modes of behavior, depending on the number of real positive equilibrium points that they have. A method is described and illustrated for reallocating attrition as state variables approach zero in order to guarantee their non-negativity.

20 DISTRIBUTION/AVAILABILITY OF ABSTRACT ☒ UNCLASSIFIED/UNLIMITED ☐ SAME AS RPT ☐ DTIC USERS	21 ABSTRACT SECURITY CLASSIFICATION UNCLASSIFIED
22a NAME OF RESPONSIBLE INDIVIDUAL P. H. Moose	22b TELEPHONE (Include Area Code) (408) 646-2838	22c OFFICE SYMBOL 62Me

DD FORM 1473, 84 MAR
83 APR edition may be used until exhausted
All other editions are obsolete.

SECURITY CLASSIFICATION OF THIS PAGE
UNCLASSIFIED

TABLE OF CONTENTS

Characteristic Trajectories
of
Generalized Lanchester Equations

by

John M. Wozencraft
Paul H. Moose

ABSTRACT

Generalized Lanchester-type differential equations are used to model attrition processes. This system of non-linear equations has multiple equilibrium solutions, which can be determined by a numerical technique called the Continuation Method when the problem's dimensionality is moderate.

System dynamics are investigated and shown to depend critically on a domain of attraction defined by a tube which connects the non-negative equilibrium points and contains the dominant eigenvector at those points. Principles are presented and illustrated for mapping NM-dimensional systems into equivalent two-dimensional systems. This capability is especially important when aggregating subsystems in multi-level systems modeling. It is shown that the two-dimensional Lanchester systems have only four distinct modes of behavior, depending on the number of real positive equilibrium points that they have. A method is described and illustrated for reallocating attrition as state variables approach zero in order to guarantee their non-negativity.

I. Introduction

Lanchester's equations were introduced during WW I to mathematically model aerial combat losses [1]. During and after WW II, they were studied extensively for their potential to model attrition over a wide variety of military combat situations [2],[3]. In their elementary form, Lanchester's equations are coupled evolution equations:

$$\dot{x}(t) = -F(x, y, t)$$
$$\dot{y}(t) = -G(x, y, t)$$

(1)

where the functions, $F(.)$ and $G(.)$ are generally non-linear in the state variables x and y. The state variables represent the size, or strength, of the opposing forces or weapons systems.

In this paper we report the results of our research into a generalized system of Lanchester equations

$$\dot{x}_i(t) = F_i(x_i, \underline{y}, t); \qquad i = 1, 2, \ldots N$$
$$\dot{y}_j(t) = G_j(\underline{x}, y_j, t); \qquad j = 1, 2, \ldots M$$

(2)

in which N components of a non-homogeneous "X-force" engage M components of a "Y-force." Motivation for this research stemmed from our interest in the decision & control problems faced by a modern day military commander. We needed an analytical model of the attrition process that would accomodate the great variety present in the military environment, but also one whose major dynamical features could be easily interpreted and understood. This lead us to study in detail the dynamic properties of the special $N \times M$ system

$$\dot{x}_i(t) = -u_i x_i(t) - \sum_{j=1}^{M} a_{ij} x_i(t) y_j(t) - \sum_{j=1}^{M} b_{ij} y_j(t) + r_i; i = 1, 2, \ldots N$$
$$\dot{y}_j(t) = -v_j y_j(t) - \sum_{i=1}^{N} c_{ij} x_i(t) y_j(t) - \sum_{i=1}^{N} d_{ij} x_i(t) + s_j; j = 1, 2, \ldots M$$

(3)

in which we assume the coefficients and replacements are deterministic nonnegative real constants. Each component (which may be a force type such as tanks or infantry, or a

force in a particular area such as Company A or B, etc.) has its population depleted by self losses, random or "area" firing (the bilinear terms) and direct or aimed firing (the linear coupling terms). The losses are offset by assumed steady rates of replacement, r and s. No infracide is allowed; that is components of the same side do not attrite one another.

The choice of this particular structure involving linear terms, bilinear terms $(x_i y_j)$, and constants is based on two observations. First, they are a generalization of the mixed attrition Lanchester equations with replacements

$$\dot{x}(t) = -ux(t) - ax(t)y(t) - by(t) + r$$
$$\dot{y}(t) = -vy(t) - cx(t)y(t) - dx(t) + s$$

(4)

and second, they represent the lead terms in a Taylor series expansion of (2). In the terminology of this paper, (4) corresponds to a 1×1 system.

Before explaining the behavior of $N \times M$ systems, it is valuable first to summarize the dynamic behavior of the 1×1 system. It is shown in Appendix A that four distinct modes of behavior are possible depending on whether one stable, one unstable, two or zero equilibrium points lie in the positive quadrant, where by definition an equilibrium is a point in the state space at which $\dot{x} = \dot{y} = 0$. Every 1×1 system always has two such points which may be positive, negative or complex numbers. In all cases, however, there is a "characteristic" trajectory; i.e., a phase plane curve to which <u>all</u> trajectories converge. This characteristic trajectory is very nearly a hyperbola. The direction and rate of evolution along this trajectory is determined by the equilibrium points and their eigenvalues. If two equilibrium points exist in the positive quadrant, one must be stable, the other unstable. If only one exists, it may be either stable or unstable. The equilibrium points lie on the characteristic trajectory. Four trajectories are illustrated in Figure 1, for the case of a single stable equilibrium point system.

Returning now to an $N \times M$ system, we may ask to what degree its dynamics in the aggregate are like those of a 1×1 system. Or, put conversely, can one find a 1×1
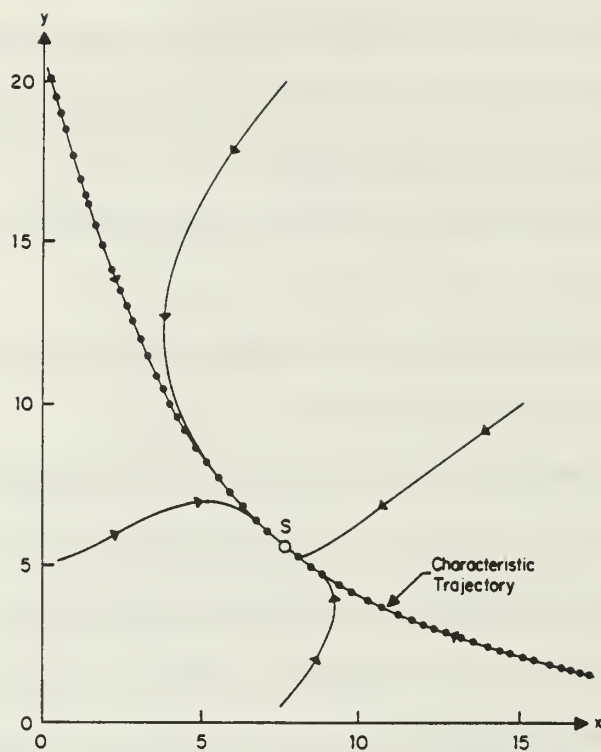
– 3–

Figure 1 - "Typical Trajectories of a 1×1 System with a Single Stable Equilibrium Point."

system whose dynamics closely resemble the aggregate behavior of an arbitrary $N \times M$ system? This is the central question to which this report is addressed.

The question is important for three reasons:

(i) The complexity of a multidimensional system grows so rapidly with the number of dimensions that it is exceedingly difficult to comprehend the nature of its dynamic behavior.

(2) Aggregation of detailed subsystems into a larger system of lower complexity provides a methodology for determining what the values of the coefficients of the larger system should be.

(iii) Aggregation permits the development of a hierarchy of models which maintains a constant degree of complexity at each level of the system.

In Appendix B we show that the general $N \times M$ system - like the 1×1 system - also has an "attractive tube" in the positive quadrant which collapses to a cone as it passes through each equilibrium point, and that these points must alternately be stable and unstable. A "characteristic trajectory", determined by the dominant eigenvector at these equilibrium points, lies inside this tube. A potential difficulty is that the general system has many equilibrium points; specifically, an $N \times N$ system has $\binom{2N}{N}$ of them, as is shown in Appendix C[4]. If more than two real equilibrium points lie in the positive quadrant, it will be impossible to find a single satisfactory 1×1 system equivalent. We conjecture, but have not proven that there are never more than two.[1]

The equilibrium points of the $N \times M$ system which lie in the positive quadrant play a critical role in determining the system dynamics. Continuation Methods [5] provide a powerful way (in principle) to find all the equilibrium points of nonlinear systems. Roots of a trivial system are tracked to the desired solution as replacement and linear

---

[1] In fact, for the numerous versions of 2×2 systems that have been investigated in this research, no more than 2 positive equilibrium points have ever occurred.

terms are introduced incrementally. This procedure is described in detail in Appendix C and illustrated for the six roots of a 2×2 system. Because we cannot tell a priori which trivial roots will become positive final roots, all must be tracked, which unfortunately limits applicability of the method to systems with moderate dimensionality.

The remainder of this paper is organized as follows: In Section II, aggregate system trajectories are presented for four 2×2 systems, along with their asymptotes, equilibrium points and eigenvalues. The four systems selected for study have equilibrium point configurations in the positive quadrant that correspond to the four types of 1×1 systems described in Appendix A. In Section III, equivalent 1×1 systems are found using mapping-down procedures that preserve the equilibrium points and the characteristic trajectory and rate of evolution near these points. The resultant 1×1 trajectories are very close to those desired, as is the dynamic behavior throughout the entire phase plane. In Section IV, an additional nonlinearity is added to the basic equations (3) to terminate losses for vanishingly small components by redirecting "aimed" fire to the remaining targets. This corrective term terminates all phase plane trajectories at the boundaries of the positive quadrant with but minimal distortion inside the positive quadrant. In Section V the results of this research and its implications for modeling and for initial force allocation are discussed.

II. Case Studies of 2×2 Systems

Equilibrium points and their local stability are important attributes of nearly all non-linear systems. Appendix C shows how the equilibrium points of an $N \times N$ system can be found by Continuation Methods. In this method, the equilibrium points of a simplified or "trivial" $N \times N$ system are determined analytically. The solutions are then tracked to their final locations as aimed fire and replenishment rate terms are introduced incrementally.

Any resultant real equilibrium points in an "extended" positive quadrant lie on

the characteristic system trajectory, which is interior to the bounding $2N$ dimensional "tube" described in Appendix B. We define the extended positive quadrant to contain all $\underline{x}, \underline{y}$ points which component by component are greater than or equal to the vector of X asymptotes $\underline{X}_A$, and of Y asymptotes $\underline{Y}_A$. In general, these asymptotes must be found by numerically integrating the $N \times N$ equations. For the 2×2 problem, they can be found as shown in Appendix D. The component asymptotes are non- positive, as are the aggregate asymptotes, defined as

$$X_A = \sum_i X_{iA} \text{ and } Y_A = \sum_j Y_{jA} \tag{5}$$

The aggregate system trajectory will be asymptotic to X_A when one component of Y's force becomes dominant, and to Y_A as one component of X's force becomes dominant.

In order to illustrate these properties, we have studied 2×2 systems in considerable detail. The Lanchester equations of the 2×2 problem are:

$$
\begin{aligned}
\dot{x}_1 &= -\left[u_1 + a_{11} y_1 + a_{12} y_2\right] x_1 - \left[b_{11} y_1 + b_{12} y_2\right] + r_1 \\
\dot{x}_2 &= -\left[u_2 + a_{21} y_1 + a_{22} y_2\right] x_2 - \left[b_{21} y_1 + b_{22} y_2\right] + r_2 \\
\dot{y}_1 &= -\left[v_1 + c_{11} x_1 + c_{21} x_2\right] y_1 - \left[d_{11} x_1 + d_{21} x_2\right] + s_1 \\
\dot{y}_2 &= -\left[v_2 + c_{12} x_1 + c_{22} x_2\right] y_2 - \left[d_{12} x_1 + d_{22} x_2\right] + s_2
\end{aligned}
\tag{6}
$$

This problem has 16 attrition coefficients, four self-attrition coefficients and four replenishment rates. It has a total of six equilibrium points. We have investigated four example systems in detail: a system with no positive equilibrium points, a system with two positive equilibrium points (one of which is stable while the other is unstable), and two systems with one equilibrium point (stable in one case and unstable in the other). The attrition coefficients selected for each of these cases are listed in Table I.

Table I

Attrition Coefficients
for Four Systems of the 2×2 Problem

$\dot{x}_1$:	u_1	a_{11}	a_{12}	b_{11}	b_{12}
Case 20	10	2	1	7	6
Case 22	10	2	1	7	6
Case 2s	10	2	1	4	5
Case 2u	3	2	1	7	6

$\dot{x}_2$:	u_2	a_{21}	b_{21}	a_{22}	b_{22}
Case 20	20	3	4	12	5
Case 22	12	3	4	12	5
Case 2s	12	3	4	6	7
Case 2u	5	3	4	12	15

$\dot{y}_1$:	v_1	c_{11}	c_{21}	d_{11}	d_{21}
Case 20	10	2	3	6	5
Case 22	10	2	3	6	5
Case 2s	10	2	3	6	5
Case 2u	10	2	3	16	6

$\dot{y}_2$	v_2	c_{12}	c_{22}	d_{12}	d_{22}
Case 20	15	2	2	4	3
Case 22	15	2	2	4	3
Case 2s	15	2	2	4	3
Case 2u	15	2	2	15	12

(Case 20 = No Equilibrium; Case 22 = Two Equilibria; Case 2s = One Stable Equilibrium; Case 2u = One Unstable Equilibrium.)

The equilibrium points and replenishment rates for each of the 2×2 systems are listed in Table II. Only the positive quadrant real equilibrium points are given.

Table II

Equilibrium Points and Replenishment Rates
for Four Systems of the 2×2 Problem

$\underline{X}$:	x_1	x_2	X	r_1	r_2	R
Case 20	-	-	-	17	20	37
Case 22(u)	2	2	4	77	117	194
(s)	4.87	5.01	9.88			
Case 2s	2	2	4	65	105	170
Case 2u	2	2	4	63	133	196

$\underline{Y}$	y_1	y_2	Y	s_1	s_2	S
Case 20	-	-	-	82	83	165
Case 22 (u)	3	3	6	82	83	165
(s)	0.79	1.39	2.18			
Case 2s	3	3	6	82	83	165
Case 2u	3	3	6	104	123	227

Here, $X = x_1 + x_2$, with Y, R and S defined similarly. The rationale for these particular attrition and replenishment values was to create in a 2×2 environment all four types of positive quadrant equilibrium points that occur in 1×1 systems. In presenting these four cases, we are looking toward Section III in which 1×1 equivalents will be determined and their dynamical behavior compared to the 2×2 aggregate dynamics.

The asymptotes of the 2×2 problem for each system are listed in Table III. They have been calculated in accordance with the procedures developed in Appendix D. Also shown are the dominant (exponentially growing) force components.

Table III

Asymptotes and Dominant Components
for the Four Systems of the 2×2 Problem

	X_{1A}	X_{2A}	X_A	Dominant y_j
Case 20	-3.5	-4	-7.5	y_1
Case 22	-3.5	-4	-7.5	y_2
Case 2s	-2	-2	-4	y_1
Case 2u	-3.5	-4	-7.5	y_1

	Y_{1A}	Y_{2A}	Y_A	Dominant x_i
Case 20	-5/3	-3/2	-19/6	x_2
Case 22	-5/3	-3/2	-19/6	x_2
Case 2s	-5/3	-3/2	-19/6	x_2
Case 2u	-2	-6	-8	x_2

Finally, in Table IV we list the largest eigenvalue and the aggregate slope of the corresponding eigenvector at each equilibrium point. The aggregate slope of the eigenvector is defined as follows: if ξ_i are the X components of the eigenvector and η_j the Y components, then the slope is $\left[\sum_j \eta_j\right] / \left[\sum_i \xi_j\right]$ in the aggregated 2 dimensional space.

Table IV

Eigenvalues and Eigenvector Slopes
for the Four Systems of the 2×2 Problem

	λmax	Aggregate Slope	X	Y
Case 20	-	-	-	-
Case 22(u)	0.731	-1.027	4	6
(s)	-0.620	-.400	9.88	2.18
Case 2s	-1.78	-1.168	4	6
Case 2u	12.62	-1.091	4	6

From the data presented in Tables I through IV, we can establish the asymptotes

of the aggregate characteristic trajectory for X versus Y, the equilibrium points (if any) through which it must pass and the slope of the trajectory at the equilibrium points. These data are shown in Figures 2 through 5. In addition, the characteristic trajectories are shown in each Figure along with important boundary trajectories, all determined by integrating the equations numerically.

The boundary trajectories are particularly important to a military commander. Figure 2 shows the boundary trajectory that marks the amount of force X must use to initiate the combat if he is to eliminate Y entirely before Y begins to dominate the conflict and eliminate X. Figure 3 indicates the presence of two boundary surfaces: one which X must exceed if he is to eliminate Y prior to the conflict stagnating at the stable equilibrium point, and one Y must exceed if he is to avoid stagnation. Figure 4, which has a single stable point, has bounding surfaces similar to Figure 3. Figure 5, which has a single unstable point, has a single boundary surface, similar to Figure 2, which divides the state space into two regions, one in which Y dominates and the other in which X dominates.
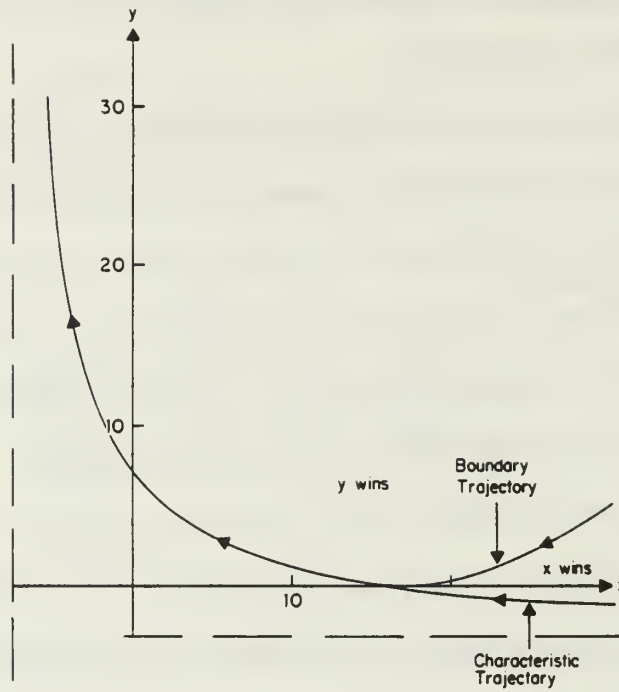
Figure 2 - "Characteristic Aggregate Trajectory and Boundary Curve for a 2×2 System with No Equilibrium Points."
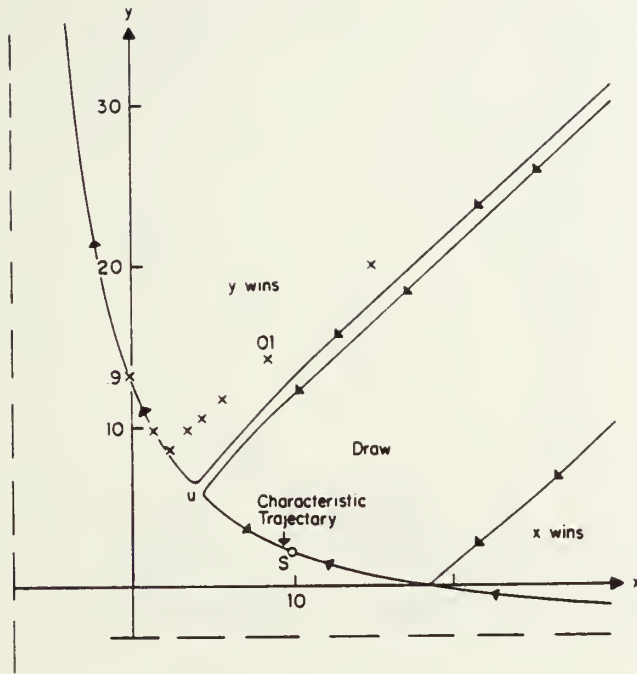
Figure 3 - "Characteristic Aggregate Trajectory and Boundary Curves for a 2×2 System with Two Equilibrium Points."
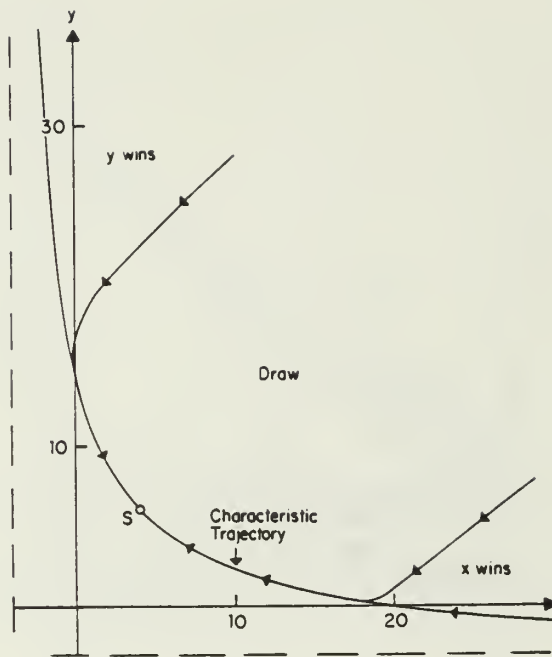
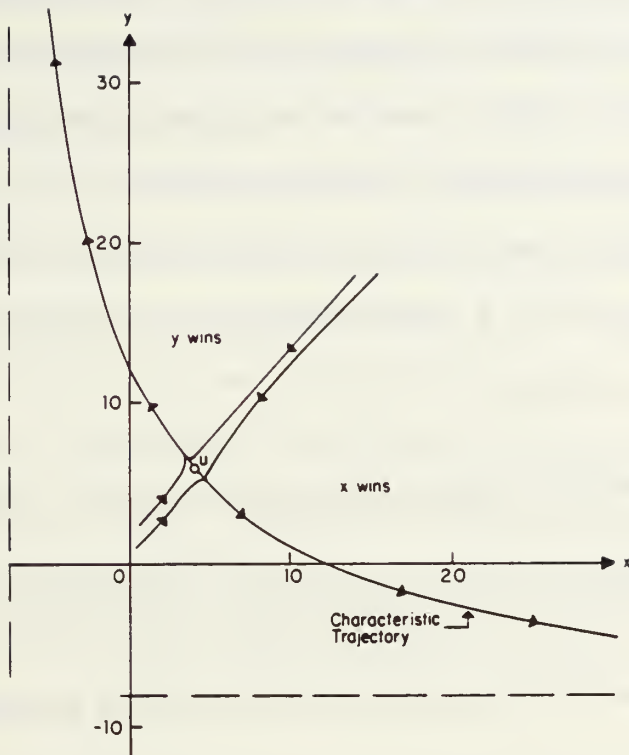Figure 4 - "Characteristic Aggregate Trajectory and Boundary Curve for a 2 × 2 System with a Single Stable Equilibrium Point."

Figure 5 - "Characteristic Aggregate Trajectory and Boundary Curve for
a 2 × 2 System with a Single Unstable Equilibrium Point."

II. Aggregation of Model

The dimensionality and number of parameters needed to characterize an $N \times N$ system, $2N(2N+1)$ attrition coefficients and $2N$ replenishment rates, make it very difficult to visualize or portray graphically the essential nature of the conflict dynamics when N is large. On the other hand, a 1×1 system is relatively easy to portray, while its four principal variations still provide variety able to match a rich assortment of military engagements. There is much to be gained by determining to what degree an $N \times N$ system can be represented by an "equivalent" 1×1 system.

The major goal of the research reported here has been to develop principles that map $N \times N$ systems into 1×1 systems. Ideally, we want the mapping to preserve closely:

a.) the aggregated phase plane trajectories $X = \sum_i x_i, Y = \sum_j y_j$

b.) the tempo of the combat (i.e., the elapsed time along the trajectories), and

c.) the cumulative resources expended by each side as the conflict evolves.

If a) and b) can be satisfied by using 1×1 replenishments equal to the aggregate replenishments ($r = R, s = S$) then the third condition is automatically satisfied.

A 1×1 system has 6 attrition coefficients and two replenishment rates. As shown in Appendix A, it has two real equilibrium points (or none), each having a dominant eigenvalue and a slope for the corresponding eigenvector. These sixteen quantities are so related that specifying any eight determines the other eight. If the replenishment rates are pre- determined by the $N \times N$ problem to be the aggregate rates, then only six parameters remain free.

In addition to preserving aggregate replenishment rates we propose the following additional principles for mapping $N \times N$ systems to 1×1 systems:

1) Positive quadrant equilibrium points are mapped to aggregate equilibrium points. This is possible for zero, one, or two points, but not more than two since a 1×1 system can only have two.

2.) Dominant eigenvalues of the equilibrium points are equated.

3.) Dominant aggregated asymptotes X_A and Y_A are equated.

4.) Slopes of the eigenvectors at the equilibrium points are equated.

Principles 1, 3 & 4 assure well mapped phase-plane trajectories. Principle 2 assures that the tempo of the combat near the equilibrium points is the same.

For $N \times N$ systems with one positive equilibrium point, principles 1 through 4 along with the replenishment rates uniquely specify a 1×1 system. For $N \times N$ systems with zero equilibrium points, only principle three applies, leaving 4 parameters undetermined. For $N \times N$ systems with two equilibrium points, principles 1 through 4 determine 10 quantities, so a "best compromise" of some kind must be found.

In order to test these principles, we have used them in mapping down the 2×2 systems studied in Section II. Table V lists the parameters determined by the 2×2 systems with one equilibrium point.

Table V

Single Equilibrium Point
1×1 Systems

	x_1	y_1	X_A	Y_A	λ_1	Slope 1
Case 1s	4	6	-4	-19/6	-1.78	-1.168
Case 1u	4	6	-7.5	-8	-12.62	-1.091

These, along with R and S determine the eight attrition coefficients as listed in Table VI.

Table VI

Attrition Coefficients
of 1×1 Equivalent System

	u	v	a	c	$(b = -X_A a)$	$(d = -Y_A c)$
Case 1s	16.06	11.70	2.65	2.58	10.60	8.17
Case 1u	4.33	11.91	2.59	2.77	19.41	22.16

The characteristic trajectory and bounding trajectories of these two 1×1 systems are shown as Figures 6 and 7. Comparisons with Figure 4 and 5 indicate that the proposed mapping principles work extremely well for 2×2 systems with single equilibrium points.

For systems with 2 equilibrium points, application of all four principles determines 10 quantities. There are only six free parameters in the 1×1 system, so a best overall fit must be found. We have elected to map the equilibrium points exactly and then find a compromise between the eigenvalues and asymptotes to produce a fit close both to the rate of conflict evolution and the phase plane geometry. (The slopes at the equilibrium points are tightly constrained by the geometry of the problem and therefore tend to be
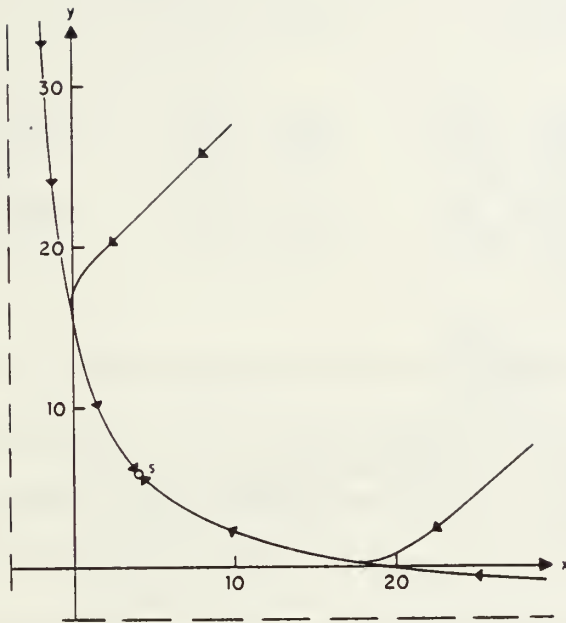
Figure 6 - "Characteristic Trajectory and Boundary Curves for an "equiv-

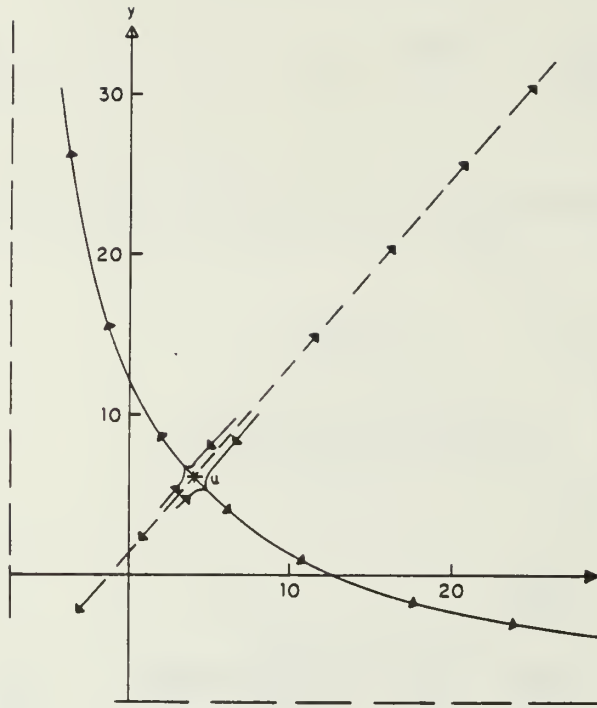alent" 1 × 1 System with a Single Unstable Equilibrium Point."

Figure 7 - "Characteristic Trajectory and Boundary Curve for an "equiv-
alent" 1×1 System with a Single Unstable Equilibrium Point."

numerically close to the desired slopes automatically). Table VII lists the properties of the 2×2 system with two equilibrium points and an equivalent 1×1 system. Characteristic phase-plane trajectories are shown in Figure 8.

<div align="center">

Table VII
Case 12
Compromise Mapping of Two Equilibrium Point System

</div>

	2×2 System	1×1 System
x_1, y_1	4,6	4,6
λ_1, slope$_1$	0.731, -1.027	0.733, -1.031
x_2, y_2	9.912, 2.18	9.912, 2.18
λ_2, slope$_2$	-.62, -.401	-.68, -.400
X_A, Y_A	-7.5, -3.1667	-6.736, -3.695

Comparing Figure 8 to Figure 3 shows that the phase plane geometries are nearly identical in the positive quadrant. The trajectories shown by x's in Figures 8 and 3 compare the tempo of combat along a particular trajectory. Again, it can be seen that these compare favorably during both rapidly evolving stages and slowly evolving stages.

Systems with zero equilibrium points are undetermined by our principles as only two values, the asymptotes, are known. Case 22 of the previous section was determined from Case 20 by increasing the replenishment rates of the X forces until there were two equilibrium points in the positive quadrants. Our "equivalent" 1×1 no-equilibrium case was obtained by utilizing the attrition coefficients of Case 12 and the replenishment factors corresponding to Case 20. The resulting trajectories are shown in Figure 9. When compared with Figure 2, we see that there is a very close agreement.

One of the critical boundaries dividing the phase plane in 1×1 systems with an unstable equilibrium point is a line passing through that point and perpendicular to the characteristic curve at that point. This curve may be found in 1×1 systems by integrating backwards in time away from the equilibrium point, thereby staying on the ridge bisecting the plane. Traveling along this ridge is the only way in which a system
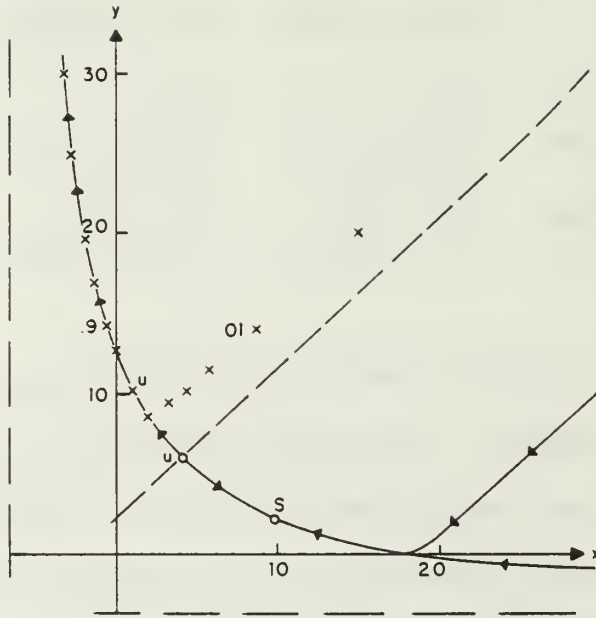
Figure 8 - "Characteristic Trajectory and Boundary Curves for an "equivalent" 1 × 1 System with Two Equilbirium Points."
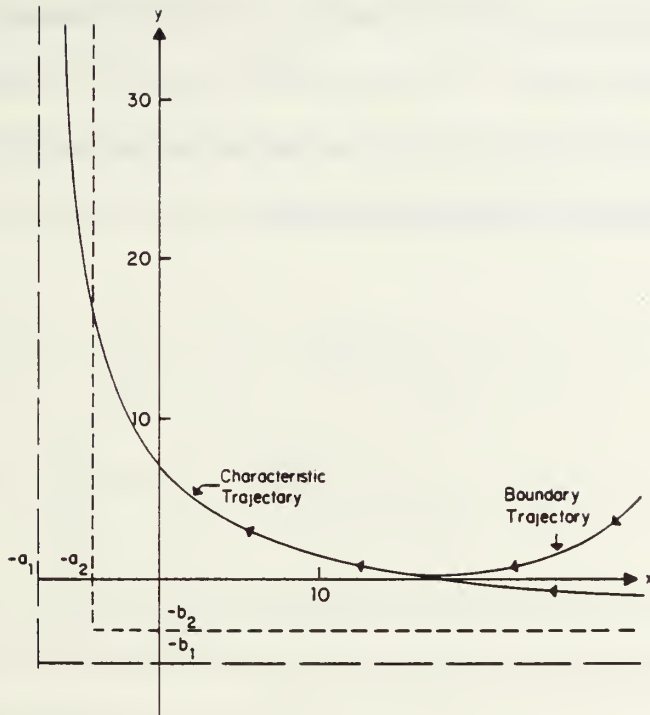
Figure 9 - "Characteristic Trajectory, Asymptotes, and Boundary Curve for an "equivalent" 1×1 System with No Equilibrium Points."

can evolve to an unstable point [6]. These bisecting curves are shown in Figures 7 and 8.

The 2×2 systems have boundary surfaces in their four dimensional state space. Therefore, aggregated boundary curves depend to some degree on the initial force compositions. All aggregated trajectories shown in Figures 2 through 5 were obtained using uniform force compositions. At least for this case, the boundaries determined by backward integration yield a very close approximation to the proper division of the aggregate state space shown in Figures 2 through 5.

IV. Terminating Attrition Losses of Vanishing Force Components

Several deficiencies exist with generalized Lanchester equations as models of combat. One of the more obvious occurs when a vanishingly small force component continues to suffer aimed fire attrition in direct proportion to the number of opposition forces. The linear attrition term is a reasonable model for aimed fire only in a "target rich" environment.

One can modify the generalized equations such that all force components will terminate at the boundaries of the positive quadrant of the state space in the following way:

$$\dot{x}_i = -x_i \left(u_i + \sum_{j=1}^{N} a_{ij} y_j \right) - \left[\frac{x_i/x_{i0}}{X/X_0} \right] \sum_{j=1}^{N} b_{i_j} y_j + r_{i_{\cdot}}; i = 1, 2, \ldots N$$

$$\dot{y}_j = -y_j \left(v_j + \sum_{i=1}^{N} c_{ij} x_i \right) - \left[\frac{y_j/y_{j0}}{Y/Y_0} \right] \sum_{i=1}^{N} d_{ij} x_i + s_j; j = 1, 2, \ldots N$$

(7)

where $X = \sum_{i=1}^{N} x_i$, $Y = \sum_{j=1}^{N} y_j$ and we make the further provision that $\lim_{X \to 0} x_i/X = 0$ and $\lim_{Y \to 0} y_j/Y = 0$ (The terms with subscripted zeros are initial values.)

The multiplier $\left[\frac{x_i/x_{i0}}{X/X_0} \right]$ assures that x_i cannot become negative because as it approaches zero, the aimed fire power of Y is reallocated away from the vanishing x_i targets to other components of the X force. The aggregate aimed fire loss rate remains essentially constant until there are no x targets left at all.

The corrective term introduced into (7) does not appear to alter significantly the aggregate trajectories of the original generalized Lanchester equations in the positive quadrant. Although (strictly speaking) it has introduced a complicated nonlinear coupling among like force components, the major practical effect on the trajectories is concentrated near zero force levels.

To illustrate the behavior, we first re-integrated Case 2u of the previous section including these factors, but found that the balanced equilibrium point force composition tends to cause the individual losing force components to come to zero nearly simultane-

ously anyway. Therefore, Case 2u does not provide a good illustration of the aimed fire reallocation property that has been built into the nonlinear coupling. Consequently, we altered the replenishment rates of Case 2u such that the unstable equilibrium point moves to (4,2,3,2) and designate it Case 2a. With the termination factors included it is designated Case 2b. The initial normalizing zero subscripted variables have been chosen at the unstable equilibrium point of Case 2a.

Figure 10 compares the force evolution of the four force components for the two cases. It shows how the attrition rate of x_1 and x_2 become zero simultaneously. The Y components do not grow quite so fast because of the greater residual x_i force.

Figure 11 compares the asymptotic aggregate phase plane trajectories of the two cases. It is evident how similar these are in the positive quadrant, although Case 2b can never exhibit a negative force component value. Since conflict typically terminates at an aggregate force level considerably greater than zero, (perhaps 20 - 50% of the inital force level), this equivalent 1×1 systems should have the desired property of modeling "aimed" fire combat more realistically.
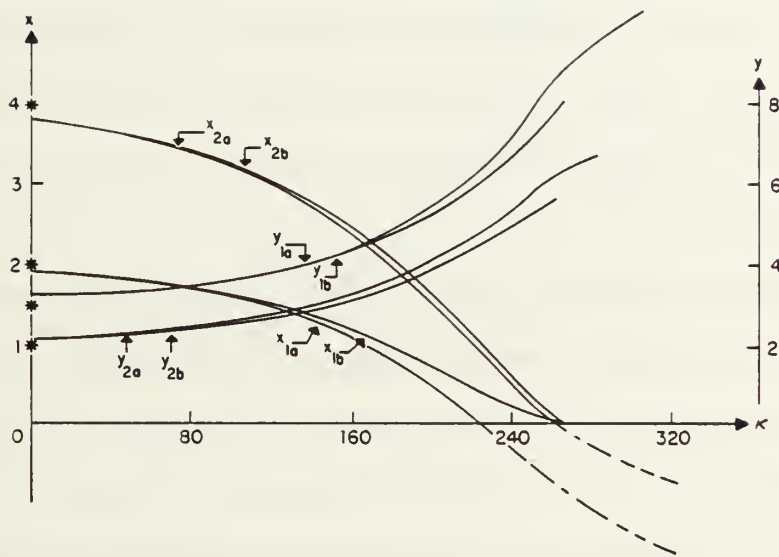
Figure 10 - "Comparing Force Component Evolution With and Without
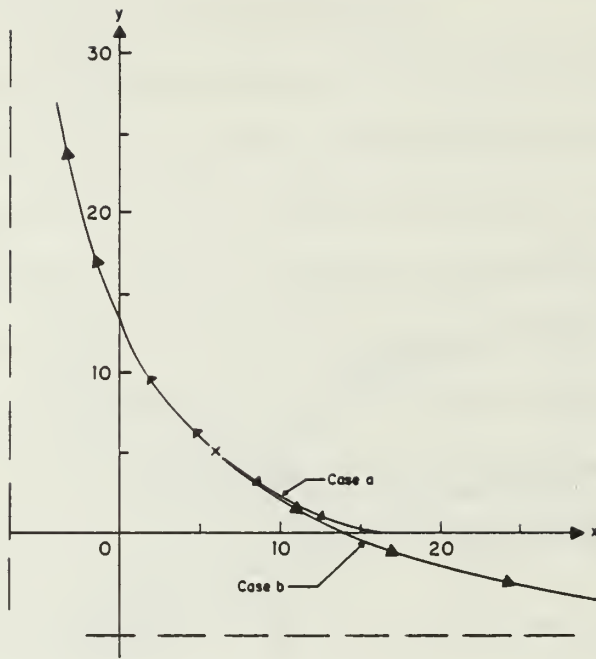Aimed Fire Reallocation."

Figure 11 - "Comparing Aggregate Phase Plane Trajectories With and Without Aimed Fire Reallocation."

V. Discussion and Further Work

In this paper we have reported the results of our research into the dynamical properties of a system of generalized Lanchester equations. The principal finding of our research is that their behavior in the aggregate is closely determined by initial conditions and a few important geometrical features in the state space. These are the equilibrium points of the system, along with their dominant eigenvalue and eigenvectors, and the asymptotes. Methods have been provided to find these features and illustrated for 2×2 systems. Given these features, one can find a characteristic aggregate trajectory toward which all trajectories are attracted. Once near this characteristic trajectory, evolution continues along it either toward an equilibrium point that is stable or away from an equilibrium point that is unstable. If there are no equilibrium points in the direction of travel, then evolution is toward an asymptote. However, since asymptotes are always negative, zero values will be reached for one or more of the state variables as the asymptote is approached. Since the state variables represent quantities of resources, evolution must be modified on approaching the boundaries of the positive quadrant. In Section IV we suggested a means to terminate the trajectories at the boundaries with minimal alteration to their properties interior to the positive quadrant.

Perhaps one of the most important results of our research is a technique to map $N \times M$ systems of Lanchester equations into equivalent 1×1 systems. There are two reasons why this is significant. First, it provides a means to determine the coefficients of large complicated systems by aggregating smaller (and simpler) ones, and to assess the sensitivity of overall system behavior to changes of individual subsystem parameters. Second, it provides a set of principles for developing a hierarchy of consistent models at ascending levels of military systems which preserves a constant level of complexity at each level. Because of the potential sensitivity of critical dynamical features (such as the eigenvalues, and hence the stability, of equilibrium points) to individual subsystem

parameters, however, it remains possible to trace their effects throughout the entire multilevel structure.

A topic of further research concerns the control of these non-linear systems. There are two controllers, one for each side, whose objectives are in conflict. Given that each side starts with finite resources and finite growth rates, then at issue is how each side should allocate his resources initially and during the evolution of the conflict. A second topic concerns the stochastic vice deterministic representation of attrition systems, as well as the effects of uncertainty in observations of the system states.

Appendix A

Asymptotes & Equilibrium Points

The 1×1 equations are:

$$\dot{x} = -ux - xay - by + r$$
$$\dot{y} = -vy - xcy - dx + s \tag{8}$$

Solving (8) for $\dot{x} = \dot{y} = 0$, we obtain

$$\left(x + \frac{b}{a}\right)\left(y + \frac{u}{a}\right) = \frac{r}{a} + \frac{b}{a} \cdot \frac{u}{a} \tag{9}$$

and

$$\left(x + \frac{v}{c}\right)\left(y + \frac{d}{c}\right) = \frac{s}{c} + \frac{v}{c} \cdot \frac{d}{c} \tag{10}$$

Each curve is a hyperbola having the form

$$(x + \alpha_i)(y + \beta_i) = (\gamma_i + \alpha_i\beta_i) \ ; \ i = I, II \tag{11}$$

the upper branches of which may be plotted as shown in Figure 12. Clearly, wherever the curves (I) and (II) cross is an equilibrium point of the differential equations. As shown in the figure there are four distinguishing cases. In cases (a) and (b) we say the asymptotes are "crossed", and there is always exactly one equilibrium point on the upper branches. In cases (c) and (d) the asymptotes are "nested"; there will be two or zero equilibrium points on the upper branches depending on the relative sizes of the terms $(\gamma_i + \alpha_i\beta_i)$.[2]

Stability at an Equilibrium Point

It is instructive to investigate the stability of (8) in the vicinity of an equilibrium point, say (x_0, y_0). Letting $x = x_0 + \delta x$, $y = y_0 + \delta y$ we have

$$\delta\dot{x} = -(u + ay_0)\delta x - (b + x_0 a)\delta y$$
$$\delta\dot{y} = -(d + cy_0)\delta x - (v + x_0 c)\delta y \tag{12}$$

---

[2] If there are no equilibrium points on the upper branches, either there are two on the lower branches or else both equilibrium points are complex. If there is one equilibrium point on the upper branches, then there is another on the lower branches.
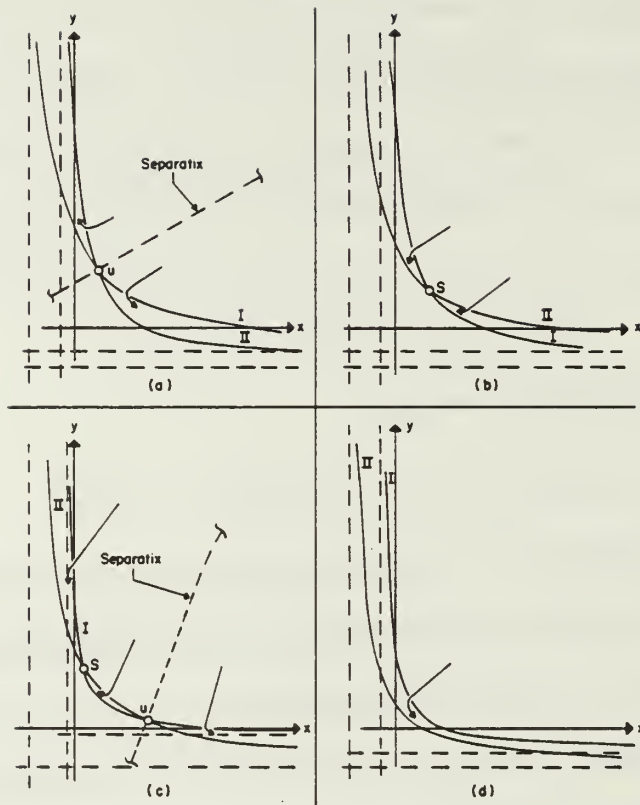
Figure 12 - "The Four Distinct Cases of the 1 × 1 Problem."

The system will be locally stable if both eigenvalues of the matrix

$$C = \begin{bmatrix} (u + ay_0) & (b + x_0a) \\ (d + cy_0) & (v + x_0c) \end{bmatrix} \tag{13}$$

have a positive real part. The characteristic equation is

$$\begin{vmatrix} (u + ay_0) - s & (b + x_0a) \\ (d + cy_0) & (v + x_0c) - s \end{vmatrix} = 0 \tag{14}$$

or

$$s^2 - (v + x_0c + u + ay_0)s + [(u + ay_0)(v + x_0c) - (d + cy_0)(b + x_0a)] = 0 \tag{15}$$

Since each term in parentheses is positive for (x_0, y_0) on the upper branches of the hyperboles (11), it follows that the real part of both eigenvalues will be positive if

$$(u + ay_0)(v + x_0c) > (d + cy_0)(b + x_0a) \tag{16}$$

If we rewrite this as

$$\frac{u + ay_0}{b + x_0a} > \frac{d + cy_0}{v + x_0c} \tag{17}$$

then from equation (12) the stability condition can be interpreted as

$$|m_x| > |m_y| \tag{18}$$

where m_x and m_y are respectively the slopes of hyperbolas I and II at (x_0, y_0).

The Trajectory Dynamics

The stability of an equilibrium point provides insight into the trajectories of combat dynamics. For large values of x and y, both $\dot{x}$ and $\dot{y}$ are negative, and a typical trajectory will move closer to the origin until it first crosses one of the hyperbolas. If in case (b) of Fig. 12 the trajectory crosses I first $\dot{x}$ becomes positive while $\dot{y}$ remains negative, and the trajectory bends towards the equilibrium point, as shown. A similar result obtains if the trajectory crosses II first: in both cases, the trajectory enters

the <u>tube</u> between I and II and heads towards the equilibrium point which is stable. Furthermore, once within the tube, the trajectory <u>cannot escape</u> since at the boundary one derivative is zero and the other points back into the tube. It follows that all 1st quadrant trajectories:

- are captured by the tube, and
- come to rest at the equilibrium point

In case (a), the equilibrium point is locally unstable. The tube between I and II again captures the trajectory, but now guides it away from the equilibrium point rather than towards it. Thus x or y will win the battle, depending on whether the initial combat point is above or below the separating curve shown in Figure 12a. This separatrix will clearly be of prime importance in any application of the theory; it can be calculated numerically (as was done for the case shown) by backwards integration from the equilibrium point, departing perpendicularly to the dominant eigenvector (which must lie within the tube.)

When there are two equilibrium points on the upper hyperbolas, it is obvious geometrically that one must be stable and the other unstable. Typical trajectories are shown in Figure 12c. If there are no equilibrium points, case (d) the tubes still capture the trajectories, and conduct them in one direction (x wins) or the other (y wins) depending on whether hyperbola I or II is uppermost.

Degenerate cases

There are two degenerate cases which we consider in the interest of completeness. If the two hyperbolas osculate, there is a double root with eigenvalue zero. The trajectories either move to the equilibrium point and stall, or else move away from it, depending upon where they enter the tube.

If the two hyperbolas coincide, the entire curve is in neutral equilibrium, so that trajectories stall at the point at which they reach the curve.

Characteristic Trajectories

The trajectory that passes through an equilibrium point along the dominant eigenvector [i.e., the eigenvector corresponding to the largest eigenvalue of the linearized equations (12)] plays a special role: we call it the "characteristic trajectory". Clearly, if the global problem were strictly linear, all trajectories ultimately would be asymptotic to the dominant eigenvector. In the bilinear case, considered here, the non-linearities appear to be sufficiently weak that the same effect occurs, and all trajectories ultimately converge onto the characteristic trajectory. The characteristic trajectory nests between the hyperbolas I and II and can itself be approximated by a hyperbola, as illustrated in Figure 13.
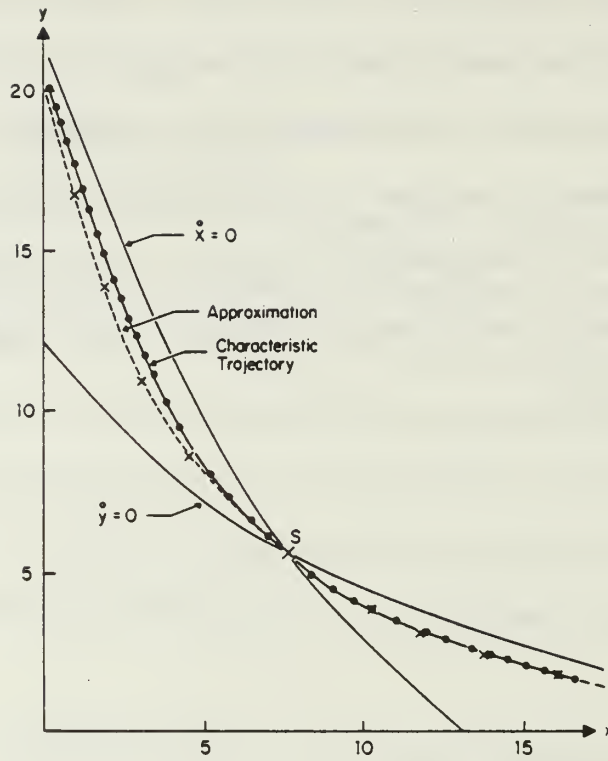
Figure 13
"A Characteristic Trajectory and its Hyperbolic Approximation."

Appendix B

Asymptotic Trajectories

In this appendix, we study the dynamics of combat evolution, primarily with the intent of understanding the nature of the multi-dimensional trajectories $\underline{x}(t), \underline{y}(t)$ when $\underline{x}$ and $\underline{y}$ are respectively N and M component vectors. The analysis is motivated by the relatively simple results in the one-by-one case, discussed in Appendix A. Our objectives are to uncover similar behavior in the $M \times N$ case, and to gain insight regarding how to aggregate multi- dimensional forces into a 1×1 model having roughly equivalent behavior.

State Equations: The combat model we analyze is a generalization of Lanchester's equations, namely:

$$\dot{x}_i = -u_i x_i - x_i \sum_j a_{ij} y_j - \sum_j b_{ij} y_j + r_i \quad ; \quad i = 1, 2, \ldots, N$$

$$\dot{y}_j = -v_j y_j - y_j \sum_i c_{ij} x_i - \sum_i d_{ij} x_i + s_j \quad ; \quad j = 1, 2, \ldots, M$$

$$(19)$$

Whenever the replenishment terms (r_j) and (s_j) exactly cancel the losses, so that all the time derivatives are zero, we have an equilibrium point, say $(\underline{x}^0, \underline{y}^0)$, and

$$x_i^0 (u_i + \sum_j a_{ij} y_j^0) + \sum_j b_{ij} y_j^0 = r_i; i = 1, 2, \ldots, N$$

$$y_j^0 (v_j + \sum_i c_{ij} x_i^0) + \sum_i d_{ij} x_i^0 = s_j; j = 1, 2, \ldots, M$$

$$(20)$$

In the vicinity of any equilibrium point, the combat evolution is governed by the set of linear equations obtained by substituting

$$x_i = x_i^0 + \delta x_i$$

$$y_j = y_j^0 + \delta y_j$$

$$(21)$$

which yields (for all i, j)

$$\delta \dot{x}_i = -\left[u_i + \sum_j a_{ij} y_j^0 \right] \delta x_i - \sum_j \left[b_{ij} + a_{ij} x_i^0 \right] \delta y_j$$

$$\delta \dot{y}_j = -\sum_i \left[d_{ij} + c_{ij} y_j^0 \right] \delta x_i - \left[v_j + \sum_i c_{ij} x_i^0 \right] \delta y_j$$

$$(22)$$

– 37–

These last equations can be written conveniently in the matrix form

$$\begin{pmatrix} \dot{\delta x} \\ \dot{\delta y} \end{pmatrix} = -C \begin{pmatrix} \delta x \\ \delta y \end{pmatrix} \tag{23}$$

where the $(N + M) \times (N + M)$ matrix C has the structure

$$C = \begin{pmatrix} & & 0 & \vdots & & & \\ & \alpha_{ii} & & \vdots & \beta_{ij} & & \\ 0 & & & \vdots & & & \\ \cdots & \cdots & \cdots & \cdots & \cdots & \cdots & \\ & & & \vdots & & & 0 \\ & \epsilon_{ij} & & \vdots & & \gamma_{jj} & \\ & & & \vdots & 0 & & \end{pmatrix} \tag{24}$$

We are interested only in situations for which $(\underline{x}^0, \underline{y}^0)$ is non-negative, in which case all the elements of (C) are non-negative.

Impermeable Boundaries: It is evident from (22) that near an equilibrium point the locus of all points on which any particular $\delta \dot{x}_i$ is equal to zero is an $(M+1)$-dimensional plane; specifically

$$\delta \dot{x}_i = 0 \quad \to \quad -\alpha_{ii} \delta x_i - \sum_j \beta_{ij} \delta y_j = 0 \tag{25}$$

Thus the point $(\delta x_i, \delta \underline{y})$ is beneath this plane if $\delta \dot{x}_i > 0$, and conversely $\delta \dot{x}_i < 0$ for all points above the plane.

We now make the simple but crucial observation that in the linearized model:

If $\delta \dot{y}_j(t) \geq 0$ for all j & t, then any point that lies beneath the plane $\delta \dot{x}_i = 0$ at $t = t_0$ will remain beneath the plane for all $t > t_0$. An easy way to verify this is to note from (22) that if at any instant t_k the point $(\delta x_i, \delta \underline{y})$ lies on the plane $\delta \dot{x}_i = 0$, then the facts

$$\delta \dot{x}_i = 0, \delta \dot{y}_j \geq 0 \text{ (for all } j)$$

imply that δx_i is (instantaneously) constant, whereas by assumption all the $\{\delta y_j\}$ either increase or are also constant. It follows that at time $t_k + dt$

$$\delta \dot{x}_i \leq 0$$

which implies that $(\delta x_i, \delta \underline{y})$ must again lie on or beneath the plane. Since the point can never penetrate the boundary plane from below, obviously it can never get above it.

Similar arguments lead to the additional cases summarized below:

$$\text{If for all } j \quad \{\delta \dot{y}_j \geq 0\}, \text{ then } \quad \delta \dot{x}_i \leq 0 \quad \text{endures for any } i$$

$$\text{If for all } j \quad \{\delta \dot{y}_j \leq 0\}, \text{ then } \quad \delta \dot{x}_i \geq 0 \quad \text{endures for any } i$$

$$\text{If for all } i \quad \{\delta \dot{x}_i \geq 0\}, \text{ then } \quad \delta \dot{y}_j \leq 0 \quad \text{endures for any } j$$

$$\text{If for all } i \quad \{\delta \dot{x}_i \leq 0\}, \text{ then } \quad \delta \dot{y}_j \geq 0 \quad \text{endures for any } j$$

We conclude that the cone in our $N \times M$ (linearized) space for which either

$$\{\delta \dot{y}_j \geq 0\} \quad \text{and} \quad \{\delta \dot{x}_i \leq 0\} \quad \text{for all } i, j$$

or

$$\{\delta \dot{y}_j \leq 0\} \quad \text{and} \quad \{\delta \dot{x}_i \geq 0\} \quad \text{for all } i, j$$

is a "trap" from which the operating point $(\delta x, \delta y)$ can not escape. Since the cone always exists, so does the trap.

The Non-Linear Case: The real problem posed by (19) differs from the incremental case (22) primarily in that the state equations are non- linear. For any fixed value of x_i, however, the locus of $\dot{x}_i = 0$ is still a plane in the (y_j); we have from (19) that

$$\dot{x}_i = 0 \rightarrow \sum_j (b_{ij} + a_{ij} x_i) y_j = r_i - u_i x_i$$

The situation may be visualized as shown in Figure 14 for the case $N = 1$ and $M = 2$. For $\dot{x}_1 = 0$, we require

$$(b_{11} + a_{11} x_1) y_1 + (b_{12} + a_{12} x_1) y_2 = r_1 - u_1 x_1$$

so that

$$y_2 = 0 \qquad \rightarrow y_1 = \frac{r_1 - u_1 x_1}{b_{11} + a_{11} x_1}$$

which is a hyperbola with asymptotes at $y_1 = -u_1/a_{11}$ and $x_1 = -b_{11}/a_{11}$, and

$$y_1 = 0 \qquad \rightarrow y_2 = \frac{r_1 - u_1 x_1}{b_{12} + a_{12} x_1}$$

which is a hyperbola with asymptotes at $y_2 = -u_1/a_{12}$ and $x_1 = -b_{12}/a_{12}$. The surface $\dot{x}_1 = 0$ is generated by the straight lines joining points on the two hyperbolas corresponding to the same value of x_1, as shown in Figure 14.

It is worth noting that the slope of the generating lines is

$$\frac{\Delta y_1}{\Delta y_2} = \frac{b_{12} + a_{12} x_1}{b_{11} + a_{11} x_1}$$

which varies from b_{12}/b_{11} at $x_1 = 0$ to a_{12}/a_{11} as $x_1 \rightarrow \infty$. By contrast, the slope of the corresponding lines in the incremental case (2) is constant. The obvious effect of the non-linearity is a "twisting" of the surfaces $\{\delta \dot{x}_i = 0\}$; the amount of twisting is, however, limited to $\leq 90^o$ by the non-negativity of the attrition coefficients.

A second observation is that the surfaces $\dot{x}_i = 0$ and $\dot{y}_j = 0$ preserve their identity throughout the (extended) positive quadrant, defined by the positive branches of the hyperbolas. Thus the twisting of these surfaces causes the trapping cone near an equilibrium point to deform into a non-linear "tube", but can neither destroy the existence of the trapping region nor change its nature. Indeed, the only way this tube can vanish is for it to contract into another cone at a second equilibrium point, and of course the tube then continues on the other side (with reversed $\delta \dot{x}_i$'s and $\delta \dot{y}_j$'s) as the cone passes through the equilibrium point. We conclude that such a tubular trap must always exist.[3] Moreover, evidently it is unique, i.e., only one such tube can exist in the extended positive quadrant.

---

[3] The tube exists even when there is no equilibrium point in the extended positive quadrant, a fact which may be deduced (for example) by reducing all r's by a scale factor (keeping all other parameters constant) until an equilibrium point does exist.
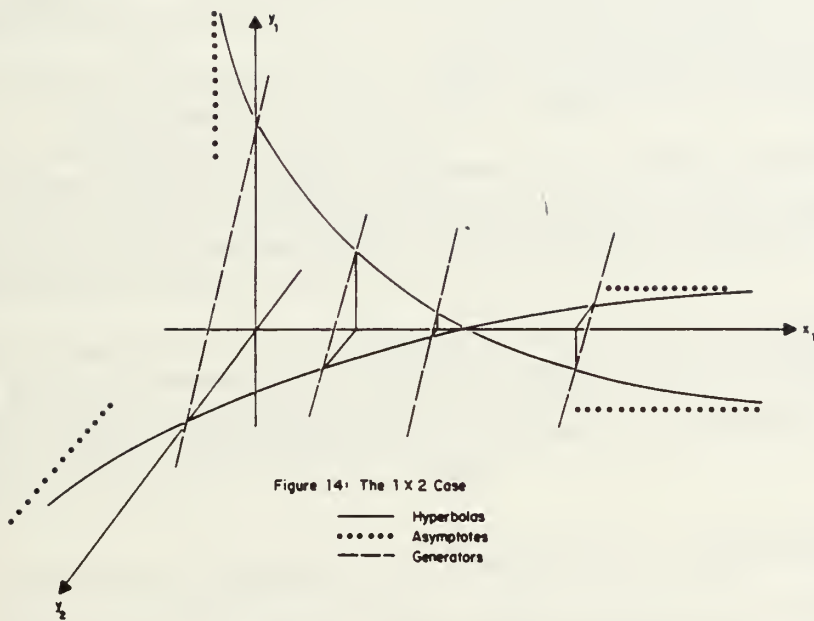
Figure 14: The 1 X 2 Case

——— Hyperbolas
•••••• Asymptotes
— — — Generators

Figure 14 - "The Attracting Tube for the 1 × 2 Problem."

Implications: A number of conclusions follow from the preceding analysis. With regard to the cones emanating from any equilibrium point, we note that:

(1) The dominant eigenvector[4] of the matrix -C in (24) must lie <u>inside</u> the trapping cone, because in the linear case any trajectory must ultimately converge onto the dominant eigenvector.

(2) All (δx_i) components of the eigenvector must have the same sign, and be opposite in sign to all the (δy_j) components because all the time derivatives have this property and no trajectory can escape the cone.

(3) All trajectories in the vicinity of the cone will be attracted into it, because it contains the dominant eigenvector.

Shifting our attention to the non-linear trapping tube, we note that:

(4) All equilibrium points in the extended positive quadrant must lie along the tube, because there can only be one tube and each equilibrium point generates a cone.

(5) The equilibrium points along the tube must alternate between stable and unstable, because all $\delta \dot{x}_i$ and $\delta \dot{y}_j$ in a cone lead either towards or away from the apex.

(6) The trapping tube is an attractor, and we strongly surmise that all trajectories originating in the extended positive quadrant ultimately approach the trajectory generated by the dominant eigenvector at any cone. Although we have as yet no formal proof for this asymptotic property, its validity is consistent with geometrical similarity to the linearized model and accords with our computational data.

---

[4] By "dominant eigenvector" we mean the eigenvector corresponding to the largest eigenvalue of -C

Appendix C

Equilibrium Solutions

In this appendix, we describe a technique to find the equilibrium points of $N \times N$ Lanchester systems. Specifically, we seek solutions of the equations

$$x_i \left(u_i + \sum_{j=1}^{N} a_{ij} y_j \right) + p \left(\sum_{j=1}^{N} b_{ij} y_j - r_i \right) = 0; i = 1, 2, \ldots, N$$

$$y_j \left(v_j + \sum_{i=1}^{N} c_{ij} x_i \right) + p \left(\sum_{i=1}^{N} d_{ij} x_i - s_j \right) = 0; j = 1, 2, \ldots, N$$

$$(26)$$

with the parameter $p = 1$. One can find them using continuation techniques, by numerically tracking the roots for $p = 0$, which are called the trivial solutions, as p is increased incrementally from zero to one.

Here, we describe how to find the trivial roots and a technique to track them to their final values, and illustrate this with data from the 2×2 examples in the paper. It is important that terms are so parameterized that there are as many trivial roots as there are final roots. This is assured by parameterizing only linear and constant terms.

It is also important that the trivial system

$$x_i \left(u_i + \sum_{j=1}^{N} a_{ij} y_j \right) = 0; i = 1, 2, \ldots, N$$

$$y_j \left(v_j + \sum_{i=1}^{N} c_{ij} x_i \right) = 0; j = 1, 2, \ldots, N$$

$$(27)$$

have readily determined solutions. One solution exists for all x_i and y_j equal to 0. Another solution exists when

$$\left(u_i + \sum_{j=1}^{N} a_{ij} y_j \right) = 0; i = 1, 2, \ldots, N$$

$$\left(v_j + \sum_{i=1}^{N} c_{ij} x_i \right) = 0; j = 1, 2, \ldots, N$$

$$(28)$$

These are simple systems of linear equations with unique non-zero solutions, providing they are linearly independent.

Other unique solutions are found by setting various combinations of the x_i and y_j, but not all of them, to zero. For example, letting x_N and y_N equal zero we have

$$x_i \left(u_i + \sum_{j=1}^{N-1} a_{ij} y_j \right) = 0; i = 1, 2, \ldots, N-1$$

$$y_j \left(v_j + \sum_{i=1}^{N-1} c_{ij} x_i \right) = 0; j = 1, 2, \ldots, N-1$$

(29)

For the remaining x_i and y_j not necessarily zero, we must have the two systems of $N-1$ linear equations in the brackets equal to zero. In general, there is one unique solution to these equations providing they too are linearly independent.

For $x_i = 0$, there are $\binom{N}{1} = N$ possible y_j's to select as zero. Since this is true for each of the $\binom{N}{1}$ choices of the x_i to be zero, there are $\binom{N}{1}^2 = N^2$ trivial solutions with exactly one x_i and one $y_j = 0$.

We may now take any two of the x_i's $= 0$ and any two y_j's $= 0$, leaving two systems of $N-2$ linear equations in brackets that must equal zero. For each pair of x_i's, there are $\binom{N}{2}$ ways of picking pairs of y_j's equal zero. This can be repeated for each way of picking pairs of x_i's $= 0$ or $\binom{N}{2}$ times. Thus there are $\binom{N}{2}^2$ solutions with exactly two x_i's and two y_j's equal zero.

This procedure can be repeated, picking $3, 4, \ldots, \ldots, N-1$ x_i's and y_j's simultaneously equal zero and solving the remaining sets of linear equations. There are $\binom{N}{k}$ ways of picking k y_j's equal zero for each set of k x_i's $= 0$. This can be repeated $\binom{N}{k}$ times for each way of picking k x_i's $= 0$, thus producing $\binom{N}{k}^2$ solutions with exactly k x_i's and k y_j's equal zero.

We can not in general obtain solutions by taking different numbers of x_i's and y_j's equal zero. This may be illustrated as follows. Suppose we take $x_N = 0$ but not, in

general, any of the y_j's. From (27), we must have

$$\left(v_j + \sum_{i=1}^{N-1} c_{ij} x_i\right) = 0 \qquad\qquad j = 1, 2, \ldots, N \qquad (30)$$

which cannot be consistent (unless they are linearly dependent) since there are N equations to satisfy with $N - 1$ variables. A similar argument pertains any time we attempt to put an unequal number of x_i's and y_j's to zero. Thus we see that there are at most[5]

$$Q = 1 + \binom{N}{1}^2 + \binom{N}{2}^2 + \cdot + \binom{N}{N}^2 = \sum_{k=0}^{N} \binom{N}{k}^2 = \binom{2N}{N} \qquad (31)$$

unique solutions to (27). Table VIII below shows the growth of trivial solutions for N from one to ten.

Table VIII

Equilibrium Solutions

N	1	2	3	4	5	6	7	8	9	10
Q	2	6	20	70	252	924	3432	23870	48620	184756

By way of illustration, consider the trivial solutions of the 2×2 problem. The

---

[5] See C. L. Liu, Introduction to Combinational Mathematics, McGraw-Hill, 1968, pp. 27 - 28, for proof of the identity

trivial equations are:

$$x_1(u_1 + a_{11}y_1 + a_{12}y_2) = 0$$

$$x_2(u_2 + a_{21}y_1 + a_{22}y_2) = 0$$

$$y_1(v_1 + c_{11}x_1 + c_{21}x_2) = 0$$

$$y_2(v_2 + c_{12}x_1 + c_{22}x_2) = 0$$

and the six solutions are

(1) $\qquad x_1 = x_2 = 0, y_1 = y_2 = 0$

(2) $\qquad x_1 = 0, x_2 = -v_2/c_{22}, y_1 = 0, y_2 = -u_2/a_{22}$

(3) $\qquad x_1 = 0, x_2 = -v_1/c_{21}, y_1 = -u_2/a_{21}, y_2 = 0$

(4) $\qquad x_1 = -v_2/c_{12}, x_2 = 0, y_1 = 0, y_2 = u_1/a_{12}$

(5) $\qquad x_1 = -v_1/c_{11}, x_2 = 0, y_1 = -u_1/a_{11}, y_2 = 0$

plus the solution to the equations

(6) $\qquad v_1 + c_{11}x_1 + c_{21}x_2 = 0, \qquad u_1 + a_{11}y_1 + a_{12}y_2 = 0$

$\qquad\qquad v_2 + c_{12}x_1 + c_{22}x_2 = 0, \qquad u_2 + a_{21}y_1 + a_{22}y_2 = 0$

We note that all solutions of the trivial system (27) are real and, except for the all zero root, have at least one negative component. The only equilibrium points of the Lanchester system ($p = 1$) that are physically significant are real points with all non-negative components. Unfortunately, one does not know which trivial roots, if any, correspond to final real, positive ones. Therefore all must be tracked, and as p increases from zero, provisions must be made for them to become complex, and once complex, to become real again as p increases even further. Note also that since the coefficients of (26) are real, complex roots occur in conjugate pairs.

A general technique of tracking the roots involves a combination of "predictor" and "corrector" steps. For the particular parameterization we have selected, these two steps are remarkably similar, each requiring solution of linear equations which differ only in their right hand sides.

We first describe the predictor step. The solutions of (26) obviously depend on p. If we perturb p, we expect a perturbation in the solution. Thus perturbing (26) by δp and retaining only first order perturbation terms in the state vector gives

$$\delta x_i \left(u_i + \sum_j a_{ij} y_j \right) + x_i \left(\sum_j a_{ij} \delta y_j \right) + \delta p \left(\sum_j b_{ij} y_j - r_i \right) + p \left(\sum_j b_{ij} \delta y_j \right) = 0$$

$; i = 1, 2, \ldots, N$

$$\delta y_j \left(v_j + \sum_i c_{ij} x_i \right) + y_j \left(\sum_i c_{ij} \delta x_i \right) + \delta p \left(\sum_i d_{ij} x_i - s_j \right) + p \left(\sum_i d_{ij} \delta x_i \right) = 0$$

$; j = 1, 2, \ldots, N$

$$(32)$$

which is recognized as a system of $2N$ linear equations in the perturbations vectors $\underline{\delta x}$ and $\underline{\delta y}$ upon rewriting as

$$\delta x_i \left(u_i + \sum_j a_{ij} y_j \right) + \sum_j \left(x_i a_{ij} + p b_{ij} \right) \delta y_j = \delta p \left(r_i - \sum_j b_{ij} y_j \right) ; i = 1, \ldots N$$

$$\delta y_j \left(v_j + \sum_i c_{ij} x_i \right) + \sum_i \left(y_j c_{ij} + p d_{ij} \right) \delta x_i = \delta p \left(s_j - \sum_i d_{ij} x_i \right) ; j = 1, \ldots N$$

$$(33)$$

If $(\underline{x}, \underline{y})$ is a root at p, then $(\underline{x} + \underline{\delta x}, \underline{y} + \underline{\delta y})$ is the best linear prediction of the root at $p + \delta p$. Since $\underline{\delta x}$ and $\underline{\delta y}$ are also potentially complex, solving (33) involves solving a system of $4N$ linear real equations.

After a few predictor steps, errors begin to creep in such that the predicted root deviates from the true root. A sequence of "corrector" steps are initiated, keeping p constant, until the error is reduced to an acceptably small value, at which point prediction is resumed. In this work, we employed a generalized Newton's Method for

correction. Let

$$ex_i = x_i \left(u_i + \sum_j a_{ij} y_j \right) + p \left(\sum_j b_{ij} y_j - r_j \right) \quad ; \quad i = 1, \ldots N$$

$$ey_j = y_j \left(v_j + \sum_i c_{ij} x_i \right) + p \left(\sum_i d_{ij} x_i - s_j \right) \quad ; \quad j = 1, \ldots N$$

(34)

be $2N$ complex error terms associated with a point $(\underline{x}, \underline{y})$.

Let us expand these in a Taylor series about a current guess for a root $(\underline{x}', \underline{y}')$, which is near the true value, and retain only the first order terms. The errors are

$$ex_i = ex_i' + \frac{\partial ex_i}{\partial x_i} \delta x_i + \sum_j \frac{\partial ex_i}{\partial y_j} \delta y_j \quad ; i = 1, 2, \ldots N$$

$$ey_j = ey_j' + \frac{\partial ey_j}{\partial y_j} \delta y_j + \sum_i \frac{\partial ey_j}{\partial x_i} \delta x_i \quad ; j = 1, 2, \ldots N$$

(35)

where the partials are to be evaluated at $(\underline{x}', \underline{y}')$. We find the new point $(\underline{x}' + \underline{\delta x}, \underline{y}' + \underline{\delta y})$ by solving for $(\underline{\delta x}, \underline{\delta y})$ such that the new errors $(\underline{ex}, \underline{ey})$ are simultaneously zero. Carrying this out one obtains the $2N$ complex linear equations.

$$\delta x_i \left(u_i + \sum_j^N a_{ij} y_j' \right) + \sum_j^N (x_i' a_{ij} + p b_{ij}) \delta y_j = -ex_i' \quad i = 1, 2, \ldots N$$

$$\delta y_j \left(v_j + \sum_i^N c_{ij} x_i' \right) + \sum_i^N (y_j' c_{ij} + p d_{ij}) \delta x_i = -ey_j'; \quad j = 1, 2, \ldots N$$

(36)

which are identical to (33) except the right hand sides have been replaced by the current errors. Thus, the predictor step and the corrector step both require solution of the same system of $4N$ real linear equations.

We have programmed the root tracking equations to track all six roots of the 2×2 problem (which requires a system of 8 linear equations) and tested it for a number of cases including the four cases described in Section II of this paper. The six trivial, or initial, roots ($p = 0$) and six final roots ($p = 1$) for these are given in Table IX. At this stage, our program remains quite interactive in order to handle trajectories as

an individual component passes through a singularity or as pairs of real roots merge to a complex conjugate pair or as complex roots separate into two distinct real roots. Nevertheless, the Continuation Method does work satisfactority and we are convinced it is a straightforward, albeit computationally intensive, means to find the equilibrium points of low order Lanchester systems.

Table IX

Equilibrium Points

	Initial Roots($p = 0$)				Final Roots ($p = 1$)			
	x_1	x_2	y_1	y_2	x_1	x_2	y_1	y_2
					-4.74	-1.66	-15.2	17.7
	0	0	0	0	+j.09	+j1.31	-j12.5	-j24.2
	0	-7.5	0/R	-3	8.42	-2.37	-1.78	-1.72
Case 20	0	-3.33	-4	0	48.7	-31.9	-4.33	-3.31
	-7.5	0	0	-10	-34.0	-5.84	-4.17	3.66
	-5	0	-5	0 #1		Conjugate		
	-12.5	0	-5.6	1.2	-6.29	-.899	-23.5	17.8
	0	0	0	0	4.89	5.01	.79	1.39
	0	-7.5	0	-3	22.9	-123.	-1.80	-2.0
Case 22	0	-3.33	-4	0	85.0	-39.0	-3.70	-1.30
	-7.5	0	0	-10	-6.20	-1.53	-18.25	-248.
	-5	0	-5	0	2.	2.	3.	3.
	-12.5	5	-5.6	-1.2	-7.15	.245	-34.9	93.4

Case 2s

0	0	0	0	2.	2.	3.	3.
0	-7.5	0	-3	18.0	-141.	-1.8	-1.88
0	-3.33	-4	0	68.8	-36.3	-3.86	-1.04
-7.5	0	0	-10	9.35	-4.15	-7.51	-11.1
-5	0	-5	0	-2.	-2.	104	13.86
-12.5	5	-5.6	1.2	-5.62	-1.26	-24.3	88.2

Case 2u

0	0	0	0	2.	2.	3.	3.
0	-7.5	0	-1.25	-3.02 $+j1.00$	-2.51 $-j1.13$	-39.9 $+j18.2$	50.1 $+j3.10$
0	-3.33	-1.67	0	#2	conjugate		
-7.5	0	0	3	20.7 $+j13.6$	-17.6 $+j27.7$	.95 $+j2.16$	-2.52 $-j2.70$
-5	0	-1.5	0	-6.13	-4.53	-14.5	-42.7
-12.5	5	-1.4	-.2	#4	conjugate		

Appendix D

2×2 Asymptotes

In this appendix, we describe how to find the asymptotes of the 2×2 system

$$\dot{x}_1 = -x_1 \left(u_1 + a_{11}y_1 + a_{12}y_2\right) - \left(b_{11}y_1 + b_{12}y_2\right) + r_1$$

$$\dot{x}_2 = -x_2 \left(u_2 + a_{21}y_1 + a_{22}y_2\right) - \left(b_{21}y_1 + b_{22}y_2\right) + r_2$$

$$\dot{y}_1 = -y_1 \left(v_1 + c_{11}x_1 + c_{21}x_2\right) - \left(d_{11}x_1 + d_{21}x_2\right) + s_1 \tag{37}$$

$$\dot{y}_2 = -y_2 \left(v_2 + c_{12}x_1 + c_{22}x_2\right) - \left(d_{12}x_1 + d_{22}x_2\right) + s_2$$

At the X asymptotes $\{X_{A1}, X_{A2}\}$ either one or both components of $\underline{y}$ are increasing without bound and $\dot{x}_1 = \dot{x}_2 = 0$ so that from (37)

$$x_1 \to X_{A1} = -\frac{b_{11}y_1 + b_{12}y_2}{a_{11}y_1 + a_{12}y_2} \quad , x_2 \to X_{A2} = -\frac{b_{21}y_1 + b_{22}y_2}{a_{21}y_1 + a_{22}y_2} \tag{38}$$

Also, from (37), the growth rates of $\underline{y}$ are approaching

$$\dot{y}_1 = -\left(v_1 + c_{11}x_1 + c_{21}x_2\right)y_1$$

$$\dot{y}_2 = -\left(v_2 + c_{12}x_1 + c_{22}x_2\right)y_2 \tag{39}$$

at the asymptotes. Now if the growth time constants are different and

$$-\left(v_1 + c_{11}x_1 + c_{21}x_2\right) > -\left(v_2 + c_{12}x_1 + c_{22}x_2\right) \tag{40}$$

then y_1 will grow exponentially faster than y_2 and eventually dominate so that

$$X_{A1} = -b_{11}/a_{11}, X_{A2} = -b_{21}/a_{21} \tag{41}$$

Combining (40) with (41) implies that

$$\frac{b_{11}}{a_{11}}\left(c_{11} - c_{12}\right) + \frac{b_{21}}{a_{21}}\left(c_{21} - c_{22}\right) > \left(v_1 - v_2\right) \tag{42}$$

Thus, if (42) holds then (41) gives $\underline{X}_A$ and y_1 is the dominant y component.

Conversely, if near the asymptotes

$$-(v_2 + c_{12}x_1 + c_{22}x_2) > -(v_1 + c_{11}x_1 + c_{21}x_2) \tag{43}$$

then y_2 is growing exponentially faster than y_1 so that

$$X_{A1} = b_{12}/a_{12} \quad , \quad X_{A2} = -b_{22}/a_{22} \tag{44}$$

Combining (43) with (44) implies that

$$\frac{b_{12}}{a_{12}}(c_{11} - c_{12}) + \frac{b_{22}}{a_{22}}(c_{21} - c_{22}) > (v_2 - v_1) \tag{45}$$

Thus if (45) holds, then (44) gives $\underline{X}_A$ and y_2 is the dominant y component.

Finally, suppose near the asymptotes that y_1 and y_2 grow exponentially at the same rate, i.e. that

$$v_2 + c_{12}x_1 + c_{22}x_2 = v_2 + c_{11}x_1 + c_{21}x_2 \tag{46}$$

and so remain in a constant ratio $k = y_2/y_1$ to one another as they grow. Combining (46) with (38) means that this constant ratio k must satisfy the non-linear equation:

$$\frac{b_{11} + kb_{12}}{a_{11} + ka_{12}}(c_{11} - c_{12}) + \frac{b_{21} + kb_{22}}{a_{21} - ka_{22}}(c_{21} - c_{22}) = v_1 - v_2 \tag{47}$$

From k, we find the asymptotes as

$$X_{A1} = -\frac{b_{11} + kb_{12}}{a_{11} + ka_{12}}, \quad X_{A2} = -\frac{b_{21} + kb_{22}}{a_{21} + ka_{22}} \tag{48}$$

The Y asymptotes, $\underline{Y}_A$ are found by similar means. The results for $\underline{X}_A$ and $\underline{Y}_A$ are displayed in Table X for single dominant components.

Table X

2×2 Asymptotes

Dominant Component	Test	Asymptotes
y_1	$\frac{b_{11}}{a_{11}}\left(c_{11} - c_{12}\right) + \frac{b_{21}}{a_{21}}\left(c_{21} - c_{22}\right) > \left(v_1 - v_2\right)$	$X_{A1} = -b_{11}/a_{11}$ $X_{A2} = -b_{21}/a_{21}$
y_2	$\frac{b_{12}}{a_{12}}\left(c_{11} - c_{12}\right) + \frac{b_{22}}{a_{22}}\left(c_{21} - c_{22}\right) > \left(v_2 - v_1\right)$	$X_{A2} = -b_{12}/a_{12}$ $X_{A2} = -b_{22}/a_{22}$
x_1	$\frac{d_{11}}{c_{11}}\left(a_{11} - a_{21}\right) + \frac{d_{12}}{c_{12}}\left(a_{12} - a_{22}\right) > \left(u_1 - u_2\right)$	$Y_{A1} = -d_{11}/c_{11}$ $Y_{A2} = -d_{12}/c_{12}$
x_2	$\frac{d_{21}}{c_{21}}\left(a_{11} - a_{21}\right) + \frac{d_{22}}{c_{22}}\left(a_{12} - a_{22}\right) > \left(u_2 - u_1\right)$	$Y_{A1} = -d_{21}/c_{21}$ $Y_{A2} = -d_{22}/c_{22}$

References

[1] F. W. Lanchester, "Aircraft in Warfare: The Dawn of the Fourth Arm - No. V, The Principle of Concentration," <u>Engineering 98</u>, p. 422–423 (1914) (reprinted on pp. 2138–2148 of <u>The World Mathematics. IV</u>, J. Newman (Ed), Simon and Schuster, New York, 1956.

[2] L. Dolansky, "Present State of the Lanchester Theory of Combat," <u>Opns. Res. 12</u>, 344–358 (1964).

[3] J. G. Taylor, <u>Force-on-Force Attrition Modelling</u>, Mil Applications Section, Opns Res Soc. of Am., 1980.

[4] B. N. Ang, <u>Equilibrium Solutions, Stabilities and Dynamics of Lanchester Equations with Optimization of Initial Force Commitments</u>, MS Thesis, Naval Postgraduate School, Sept 1984.

[5] S. L. Richter and R. A. DeCarlo, "Continuation Methods: Theory and Applications," IEEE Trans. on Systems, Man, and Cybernetics, Vol. SMC- 13, No. 4, July/Aug 1983, pp. 459-464.

[6] H. Ohihiro; <u>Non-Linear Oscillations in Physical Systems</u>, McGraw-Hill, 1964.

DISTRIBUTION LIST

Naval Postgraduate School Library
Code 0142
Monterey, California 93943-5000   1

Professor M. Sovereign
Code 74 - C-3
Naval Postgraduate School
Monterey, California 93943-5000   1

Professor P. H. Moose
Code 62Me
Naval Postgraduate School
Monterey, California 93943-5000   12

Professor J. Taylor
Code 55Tw
Operations Research
Naval Postgraduate School
Monterey, California 93943-5000   1

Professor G. Howard
Code 012
Naval Postgraduate School
Monterey, California 93943-5000   1

Mr. V. Monteleon
Code 421
Naval Ocean Systems Ctr.
San Diego, CA 92152   1

Mr. James R. Bambery
Vector Research Inc.
901 S. Highland St.
Arlington, VA 22204   1

Professor Leslie G. Callahan, Jr.
7105 Duncourtney Dr., NE
Atlanta, GA 30328   1

Dr. John T. Dockery
2507 Pegasus lane
Reston, VA 22091   1

Dr. Joseph P. Fearey
NASA-CALTECH
Jet Propulsion Laboratory
4800 Oak Grove Drive
Pasadena, CA 91109   1

Mr. W. Gerber
6060 Haverhill Ct.
Springfield, VA 22152   1

Dr. Robert L. Helmbold
4505 Avamere St.
Bethesda, D 20814   1

Dr. Perry L. Studt
Lawrence Livermore National Laboratory
Mail Stop L83
P.O. Box 808
Livermore, CA 94550   1

Dr. Robert F. Wells
1910 Camino Mora
Los Alamos, NM 87544   1

Mr. Freed Feer (RAND)
22910 Portage Circle
Topanga, CA 90290   1

Dr. William Verry
Rt. 2, Box 203A
Liberty, S.C. 29657   1

Mr. Lawrence J. Low
60 Skywood Way
Woodside, CA 94062   1

Dr. Allan S. Rehm
13320 Tuckaway Dr.
Fairfax, VA 22033   1

Dr. Helmut M. Sassenfeld
TRADOC Systems Analysis Activity (TRASANA)
Bldg. 1400
White Sands Missile Range, NM 88002-5502   1

Defense Technical Information Center   2
Cameron Station
Arlington, VA 22304-6145